Talanta 120 (2014) 198–207

Contents lists available at ScienceDirect

Talanta

journal homepage: www.elsevier.com/locate/talanta

Gold nanoparticle mediated designing of non-hydrolytic sol–gel cross-linked metformin imprinted polymer network: A theoretical and experimental study

Ekta Roy [a], Santanu Patra [a], Rashmi Madhuri [a,*], Prashant K. Sharma [b]

[a] Department of Applied Chemistry, Indian School of Mines, Dhanbad, Jharkhand 826004, India
[b] Functional Nanomaterials Research Laboratory, Department of Applied Physics, Indian School of Mines, Dhanbad, Jharkhand 826004, India

ARTICLE INFO

Article history:
Received 17 September 2013
Received in revised form
26 November 2013
Accepted 26 November 2013
Available online 13 December 2013

Keywords:
Molecular imprinted polymer
Metformin
Non-hydrolytic sol–gel
Gold nanoparticles
Electrochemical sensor

ABSTRACT

A sensitive and selective electrochemical sensor based on molecularly imprinted polymers was developed for trace level detection of metformin—an antidiabetic drug. For the first time, we have applied non-hydrolytic sol–gel matrix as a cross-linking agent in the field of molecular imprinting. To create the sol–gel matrix and enhance the electro-conductivity of the proposed sensor citrate-capped gold nanoparticle were used. The morphologies and properties of the sensor were characterized by scanning electron microscopy, cyclic voltammetry, electron impedance spectroscopy, chronocoulometry and differential pulse voltammetry. Energy of the HOMO and LUMO orbitals and Mülliken's atomic charges of template molecule were also calculated using density functional theory utilizing B3LYP with 3-21G-basis set. The theoretical results allied to the diagnostic criteria of the cyclic voltammetry indicate that the metformin redox mechanism is associated to the irreversible oxidation process of metformin-imino-group to N-hydroxyimino-group. The results demonstrated that the prepared sensor had excellent selectivity and high sensitivity for metformin in the linear range from 0.02 to 80 ng ml^{-1} with a detection limit of 0.005 ng ml^{-1} ($S/N=3$). The sensor was also successfully employed to detect metformin in pharmaceutical sample.

1. Introduction

Metformin (N, N-dimethylimido dicarbonimidic diamide monohydrochloride) is an oral antidiabetic drug in the biguanide class. It is the first-line drug of choice for the treatment of type 2 diabetes, in particular, in overweight and obese people and those with normal kidney function [1]. Metformin is the only anti-diabetic drug that has been conclusively shown to prevent the cardiovascular complications of diabetes. It helps in reduction of LDL cholesterol and triglyceride levels. In 2010, World Health Organization enlisted metformin among one of the only two oral antidiabetic drugs in the model list of essential medicines [2]. Therefore, metformin is an effective antidiabetic drug for the treatment of Type II diabetes. It is necessary and important to monitor the concentrations of the drug in blood plasma and their pharmacokinetics for the optimization of dose with accuracy.

Various analytical methods have been described for the measurement of metformin in biological fluids, including high performance liquid chromatography coupled with several detectors and extraction techniques [3–5], gas chromatography (GC) with electron-capture [6], solid phase extraction [7], fast Fourier continuous cyclic voltammetry [8], voltammetry [9–12], capillary electrophoresis (CE) [13] and conductometry [14]. But the major problem associated with the detection of this drug is the high polarity of molecule. So for the metformin analysis the GC methods require a complex and time-consuming derivatization procedure [15], while CE method use an ion-pair extraction to remove ionic substances from blood plasma samples [16]. The reported HPLC methods also suffer from several disadvantages, such as lack of sensitivity [17], complex extraction procedures [18,19], use of ultrafiltration, column-switching system [20], expensive instrumentation, running costs and long chromatographic time. Therefore, a very sensitive, selective, rapid, and cost-effective technique is required for the estimation of metformin in biological and pharmaceutical samples.

Electrochemical analysis is an excellent technique for the sensitive determination of drugs and related compounds in pharmaceutical samples and biological fluids [21]. Now-a-days the popularity of electrochemical techniques in the field of drug analysis is due to their simplicity, high sensitivity, low cost, and relatively short analysis time, although it lacks selectivity.

To improve selectivity and specificity during electrochemical analysis the most popular technique is synthetic molecular recognition, which is also termed as molecularly imprinted polymers (MIP) [22]. It is a polymer network created by the appropriate combination of monomer, template and cross-linker. After polymerization,

* Corresponding author. Tel.: +91 9471191640 (R), +91 326 2235935 (O); fax: +91 326 2296563.
E-mail address: rshmmadhuri@gmail.com (R. Madhuri).

0039-9140/$ - see front matter © 2013 Elsevier B.V. All rights reserved.
http://dx.doi.org/10.1016/j.talanta.2013.11.074

the template molecule is removed from the polymer matrix, leaving behind a cavity specific to the shape and size of template molecule. The resultant MIPs exhibits high selectivity, excellent mechanical strength, durability to heat, acid and basic conditions and better engineering possibility than their biological counterparts.

Although the conventional imprinting protocol is simple and effective, there are several critical factors to overcome viz., uncontrollable random polymerization (resulting in the heterogeneity of the imprinted sites), and high cross-linking (causes slow diffusion and poor rebinding of template) [23]. In the same pursuit, we have tried to overcome all these problems of MIP by incorporation of gold nanoparticle (AuNP) and silica compound.

Till date, sol–gel materials are commonly applied either as adhesive material or in compact matrix preparation. However, in this paper, we have explored the brightest part of silica compounds i.e. in thin film preparation and as a cross-linking agent to strengthen the imprinted polymer network. For the preparation of sol–gel matrix, other than conventional hydrolytic route, non-hydrolytic sol–gel (NHSG) synthesis procedure is opted in this work. In aqueous systems, metal alkoxides are the most widely used precursors, and their chemical transformation into the oxide network involves hydrolysis and condensation reactions. In aqueous sol–gel processes the water molecules supply the oxygen for the formation of the oxide compound. In non-aqueous systems, where intrinsically no water is present, the question arises, where the oxygen for the metal oxide comes from. Analogous to the non-hydrolytic preparation of bulk metal oxide gels [24], the oxygen for nanoparticle formation is provided by the solvent (ethers, alcohols, ketones or aldehydes) or by the organic constituent of the precursor (alkoxides or acetylacetonates), herein citrate-capped AuNPs work as oxygen donor. Usually NPs are explored for their electronic, catalytic, and many more properties [25].

In this work, for the first time, we have utilized and explored dual behavior of AuNPs i.e. (1) as oxygen donor for hydrolysis and condensation of silane and (2) as enhancer for electro-conductivity. Our main aim in this work is to overcome the problem of difficult template washing from the compact imprinted polymer matrix by the combination of sol–gel synthesis and nanotechnology. Furthermore, the synthesized nanomaterial was used for the fabrication of electrochemical sensor capable of metformin detection in real sample matrix at trace level.

2. Experimental section

2.1. Reagents

Gold (III) chloride hydrate ($HAuCl_4$), tetraethyl orthosilicate (TEOS), sodium citrate, acrylic acid (AA), acrylamide (AM), 2,2′ azoisobutyronitrile (AIBN), ethylene glycol dimethyl bisacrylate (EGDMA), metformin and other interferents were purchased from Aldrich (Steinheim, Germany) and Fluka (Steinheim, Germany). Solvents, dimethyl sulphoxide (DMSO) and ethanol were procured from Spectrochem Pvt. Ltd. (Mumbai, India). Standard stock solution of metformin (5.0 mg mL^{-1}) and others were prepared by using distilled water. The analyzed pharmaceutical sample was Cetapin XR (500 mg) and was purchased from Sanofi Diabetes, India.

2.2. Apparatus

All the electrochemical analysis [cyclic voltammetry (CV), electron impedance spectroscopy (EIS), chronocoulometry and differential pulse voltammetry (DPV)] were performed on CH instrument (USA, model number 660 C), using a three electrode cell assembly consisted of a MIP-modified Pt electrode, a platinum wire, and an Ag/AgCl (3.0 M KCl) as working, counter, and reference electrodes, respectively. Morphological images of bare and modified electrode surfaces were recorded using a scanning electron microscope (SEM), Hitachi, model S-3400N. For the binding characterization IR analysis was carried out on Varian Fourier Transform Infrared [FTIR (USA)] spectrometers. For the AuNPs characterization UV analysis was performed using a Perkin Elmer Lambda 35 (Singapore) spectrophotometer. All the experiments were performed at room temperature (25 ± 1 °C) under ambient conditions.

2.3. Computational study

Gaussian 03 was used as a tool to study binding interaction between various monomers and template molecule. All the structures of monomer, template and monomer–template complex were drawn with the help of chemdraw ultra and gauss view 4.0 software. Firstly, all the structures were optimized using Hartree-Fock theory with 6-311G** basis set and were further optimized using the density functional theory (DFT) approach utilizing hybrid Becke three-parameter exchange-correlation functional (B3LYP) with 3-21G basis set. The binding energy of template–monomer complexes, ΔE, were calculated via following equation:

$$\Delta E = E(\text{template–monomer complex}) - E(\text{template}) - nE(\text{monomer}) \quad (1)$$

Based on the results obtained from computational study of monomer–template interaction final synthesis was performed. Because polymerization is occurred in solution, we must take into account the effect of solvent, during energy calculations because it leads to changes in energy and stability of the template–monomer complexes in solvent phase than gaseous phase. In this work, Polarizable Continuum Model (PCM) was applied to calculate the energy of complex. In this model solvent was taken as a uniform polarizable medium with a dielectric constant of ε, while the solute is placed in a suitably shaped cavity in the medium [26]. Herein, DMSO (dielectric constant, $\varepsilon = 46.7$) was selected for the modeling because it was used as the porogen during polymer preparation. Based on the results obtained from computational study of monomer–template interaction final synthesis was performed.

2.4. Synthesis of citrate capped-AuNPs

Citrate capped-AuNPs were synthesized using sodium citrate, following earlier reported method [27]. In brief, first of all, 250 μL of 1.0% $HAuCl_4$ was added in a 250 mL Erlenmeyer flask containing 25 mL of deionized water, and the mixture was heated with continuous stirring. To the boiling mixture, 750 μL of 1.0% sodium citrate was added followed by color changes from purple to blue and finally to wine red, indicating formation of citrate capped-AuNP. Once the AuNPs were formed, the solution was stirred for another 15 min (without heating) for the completion of the reaction. The colloidal gold solution then centrifuged at 1500 rpm and dried at room temperature to obtain citrate capped AuNPs. The characterization of AuNPs and their role in polymer synthesis are discussed in Supplementary material (SI-Section 1.1).

2.5. Synthesis of metformin imprinted polymer

Herein, various types of imprinted polymer were prepared using different concentrations of the capped-AuNPs, TEOS, monomer and template and are shown in Table 1. For the synthesis of optimized polymer (optimization of polymer composition is discussed in SI-Section 1.2), to separate solutions were prepared. Firstly, the template molecule (metformin, 0.1 mmol, 0.0129 g dissolved in 0.5 ml of DMSO) was mixed with the selected functional monomers acryl amide (0.1 mmol, 0.0071 g dissolved in 60 μL DMSO) and

Table 1
Optimization of composition of metformin-imprinted polymer.

Type of Polymer*	Amount of acryl amide (mmol)	Amount of acrylic acid (mmol)	Amount of AuNP (ml)	Amount of TEOS (mmol)	Amount of metformin (mmol)	Current (μA)**
Polymer 1	0.1	0.1	–	0.5	0.1	20.0
Polymer 2	0.1	0.1	0.25	0.5	0.1	60.0
Polymer 3	0.1	0.1	0.50	0.5	0.1	65.0
Polymer 4	0.1	0.1	0.75	0.5	0.1	35.0
Polymer 5	0.1	0.1	0.50	0.25	0.1	30.0
Polymer 6	0.1	0.1	0.50	0.75	0.1	41.0
Polymer 7	0.1	0.1	0.50	1.0	0.1	41.0
Polymer 8	0.1	0.2	0.50	0.50	0.1	45.0
Polymer 9	0.1	0.3	0.50	0.50	0.1	32.0
Polymer 10	0.2	0.1	0.50	0.50	0.1	78.0
Polymer 11	0.3	0.1	0.50	0.50	0.1	36.0
Polymer 12	0.2	0.1	0.50	0.50	0.05	42.5
Polymer 13	0.2	0.1	0.50	0.50	0.2	34.0
Polymer 14***	0.2	0.1	0.50	–	0.2	15.6
NIP	0.2	0.1	0.50	0.50	–	NA

* During polymerization AIBN is used as an initiator in which amount is 0.01 mmol.
** Synthesized polymer used to fabricate electrodes, which later on used to measure DPV current for 10 ng mL^{-1} metformin.
*** Polymer 14 is prepared in the presence of 0.5 mmol of EGDMA, the most popular cross-linker in molecular imprinting for comparison.

acrylic acid (0.2 mmol, 0.0136 ml) in a glass vial. Wheres, the sol–gel solution of TEOS was made separately by mixing and stirring of TEOS (0.5 mmol, 0.1116 ml) and 0.5 ml AuNPs (to make a water free medium for non-hydrolytic sol–gel hydrolysis, 1 mg AuNPs powder suspended in 0.5 mL ethanol was taken in the experiment) for 15 min. These two solution were mixed together followed by addition of initiator AIBN (0.01 mmol, 0.0164 g) (Schemes 1 and 2). To remove dissolved oxygen, the final solution was purged with high purity nitrogen (99.999%) for 10min. Finally, the test tube was sealed under the nitrogen atmosphere and was then placed in a pre-heated electric oven at 50 °C for 3 h. Similarly, non-imprinted polymer (NIP) and EGDMA cross-linked polymers were also synthesized. However, NIP was prepared in the absence of metformin and EGDMA cross-linked polymer was prepared using EGDMA as cross-linker in place of TEOS.

2.6. Fabrication of metformin-imprinted electrode

In order to prepare the metformin-specific sensor, 0.5 mg of adduct polymer (polymer with template) was dispersed in 50 μL of DMSO and drop coated onto the Pt-electrode surface, followed by drying at room temperature for overnight. Similarly, NIP-modified and EGDMA-cross-linked polymer-modified electrodes were also prepared to explore the role of imprinted materials and silane cross-linking. For template extraction, modified electrodes were immersed in 0.1 M NaOH solutions for 20 min. The complete template removal from electrode surface was ensured till no voltammetric transduction response was noticed.

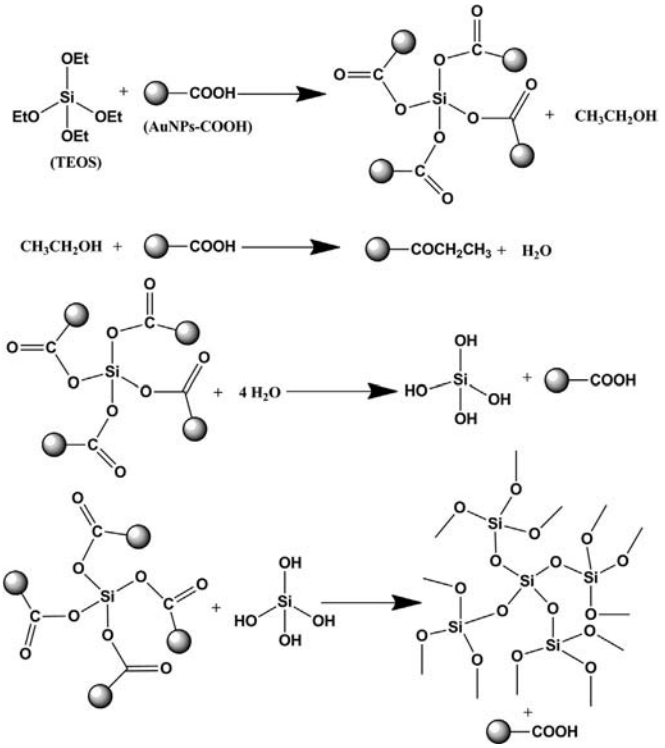

Scheme 1. Non-hydrolytic sol–gel preparation using AuNPs as oxygen donor.

2.7. Electrochemical measurement

All voltammetric measurements were performed in a cell containing 10 mL KCl solution. First of all, blank run was taken then test solution was added into the cell. After analyte accumulation for 250 s at −0.4 V vs. Ag/AgCl and 15 s equilibration times, DPV runs were recorded in the potential range varying from 0.1 V to −0.7 V (vs. Ag/AgCl) at a scan rate 10 mV s^{-1}, pulse amplitude 25 mV, and pulse width 50 ms. CV experiments were performed within the potential window +0.8 V to −0.7 V (vs. Ag/AgCl) at various scan rates (0.02–0.10 V s^{-1}). Since oxygen did not influence the oxidation of metformin, any deaeration of the cell content was not required in this experiment. All DPV runs for each concentration of test analyte were quantified using the method of standard addition. The limit of detection (LOD) was calculated as three times the standard deviation from the blank measurement (in the absence of metformin) divided by the slope of calibration plot between metformin concentration and DPV current [28]. Voltammetric measurements, as mentioned above, were also carried out on NIP- and EGDMA-cross linked polymer-modified electrodes, under the similar operating conditions.

3. Result and discussions

3.1. Theoretical study of template–monomer interactions

Molecular modeling and computational methods may aid the selection of suitable functional monomers for imprinting process. Monomers with the highest binding energies are subsequently

selected to produce MIPs with superior recognition properties. Firstly, optimization of the chemical structures of the template and monomer molecules with the calculation of the minimized energies of their respective structures was carried out. Optimized molecular structures of chosen monomers i.e. acrylamide (AM), 4-vinylpyridine (VP), methacrylic acid (MAA), acrylic acid (AA), acrylonitrile (AN), methyl methacrylate (MMA), methacrylamide (MA) and template (metformin) molecule are depicted in Fig. S1 (I–VIII). The optimized minimum energy of template, monomers and their complexes (1:1, 1:2, and 1:3) were portrayed in Supplementary material (Table S1). Herein, the computational analysis was carried out in three steps; the first step was dedicated to calculate the interaction energy between a monomer unit and template molecule i.e. a molar ratio of 1:1 (monomer:template), second for 2:1 and third was focused for 3:1 monomer:template ratio complex. Now, binding energy was calculated using the equation described earlier in Section 2.3, as we know, higher the value of interaction energy between two molecular moieties the more stable the complex formed between these moieties. Table 2 summarizes the calculated interaction energies for complexes formed between metformin and functional monomers in the gaseous as well as solution (in DMSO) phase. The obtained results reveal that the 3:1 complexes are most stable among other 1:1 and 2:1 complexes formed between the template and all the monomers tested (Fig. 1). However, in 3:1 complex between monomer and template, the 2:1:1 combination of AM, AA and metformin gives the most stable complex of monomers and template in both gaseous and solvent phase. Furthermore, in solution phase, order of interaction energy is quite similar to that obtained in gaseous phase (Table 2). This suggests that binding between monomer and template is strong enough to persist in solution phase also. Hence, this ratio is used throughout the experiment to prepare the imprinted polymer and is expected to be with highest efficiency.

3.2. Spectral characterization

The FT-IR spectra of metformin (template), adduct (with and without AuNPs) and MIP were portrayed in Fig. 2. The spectra were compared to comprehend the role of AuNPs in silane condensation mechanism (Scheme 1) and tentative binding mechanism of

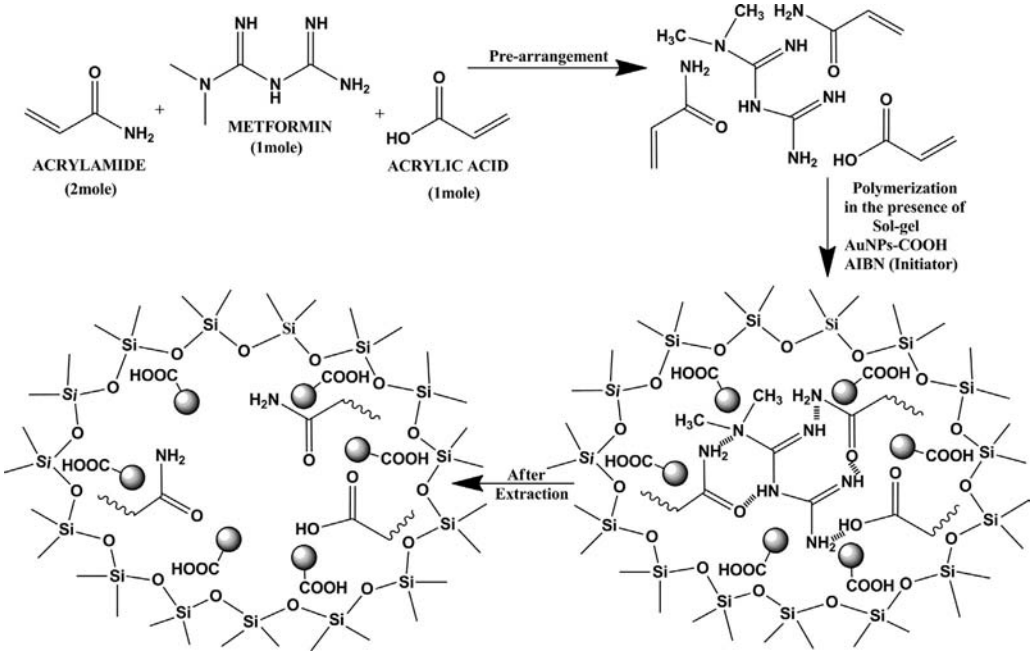

Scheme 2. Schematic representation of template and monomer interaction to form imprinted polymer network for metformin embedded in sol–gel matrix.

Table 2
Computational study of interaction energy between chosen monomer and template complex in gaseous and solvent phase.

Name of compound	In gaseous phase		In solvent phase (DMSO)	
	ΔE (Hartree)[a]	ΔE (kJ/mol)	ΔE (Hartree)[a]	ΔE (kJ/mol)
Met-Acrylic acid (AA)	−1.0300	−2704.265	−0.998	−2620.248
Met-Acrylamide (AM)	−1.0221	−2683.523	−0.984	−2583.491
Met-4-vinylpyridine (VP)	−0.2448	−642.722	−0.212	−556.605
Met-Methacrylic acid (MAA)	−0.1072	−281.453	−0.101	−265.175
Met-Acrylonitrile (AN)	−0.8387	−2202.006	−0.765	−2008.507
Met-Methyl methacrylate (MMA)	−0.3299	−866.152	−0.312	−819.155
Met-Methacrylamide (MA)	−0.8516	−2235.875	−0.768	−2016.383
Met-$(AA)_2$	−1.8082	−4747.429	−1.742	−4573.620
Met-$(AM)_2$	−2.8804	−7562.490	−2.768	−7267.382
Met-$(AA)_3$	−1.6253	−4267.225	−1.542	−4048.520
Met-$(AM)_3$	−3.3193	−8714.822	−3.219	−8452.483
Met-AM-$(AA)_2$	−3.9709	−10425.597	−3.871	−10163.309
Met-AA-$(AM)_2$	−5.2299	−13731.102	−5.130	−13468.813

[a] 1 Hartree = 2625.499 62 kJ mol^{-1}.

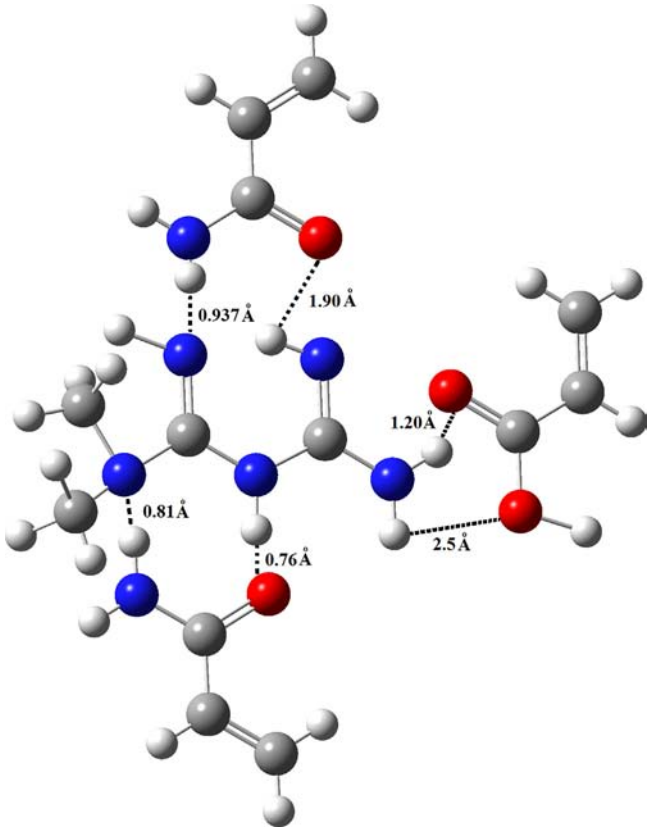

Fig. 1. Optimized geometry of the interaction complex formed between template and monomers (1:1:2).

monomer and template (Scheme 2). As depicted in spectra A and B, the frequency of –NH asymmetric and symmetric stretching, –C=N– stretching, –NH in plane deformation and –C–N–C– deformation appears at 3342, 3250, 1678, 1584 and 765 cm^{-1} for metformin but shifted to a lower wavenumber (from 3285 to 2800 and 1580, 1504 and 648 cm^{-1}) after binding with monomers (adduct) through hydrogen bonding. Interestingly, all the shifted bands of the template disappeared while polymer bands (amide-I, 1720; amide-II, 1680; –C–N–, 1420 and 1350; –C–O–, 1280; –NH wagging, 880 and 760 cm^{-1}) reinstated at their original positions, after complete template extraction (Spectrum C). To show the binding interaction of TEOS with polymer network, IR spectra of pure TEOS is also studied (Supplementary material, Fig. S2). As shown in Fig. S2, the peak due to Si–O–Si band found at 1120 and 500 cm^{-1} get shifted to 1087 and 468 cm^{-1} in both MIP and adduct. This confirms the hydrogen bonding interaction between polymer network and TEOS. To explore the role of AuNPs in the sol–gel preparation IR spectra of polymer with and without NPs were compared (Fig. 2, spectra C and D). As evident in spectrum D, no Si–O–Si band is present, which is existing in both the spectra of adduct and MIP (at 1087 and 468 cm^{-1}), suggest that condensation reaction cannot be possible without any oxygen donor and herein the role is played by citrate-capped AuNPs (Scheme 1). This is also clear from spectra that –COOH group of AA and AM, get binds with metformin molecule in polymer matrix, so not free to participate in hydrolysis of TEOS. This fact further verifies that TEOS hydrolysis fully depends up on AuNPs and –COOH group of AA does not participate in this reaction.

3.3. Morphological characterization

Surface of modified and bare electrodes were characterized by scanning electron microscopy (Fig. 3). SEM image of bare electrode shows a smooth and shining surface of Pt electrode (Fig. 3A). While comparing the morphology of electrode surface coated with adduct (template inside the polymer matrix) form in the presence of EGDMA as a cross-linker (Fig. 3B), adduct prepared with silane in the presence (Fig. 3C) and absence (Fig. 3D) of AuNPs, it is clearly visible that EGDMA cross-linked polymer network and silane without AuNPs polymer network is rough. Whereas, adduct formed in the presence of silane and AuNPs is comparatively smooth. Fig. 3E and F reveals the morphology of MIP-modified surface (after washing of template) in the presence of EGDMA and silane with AuNPs, respectively. Herein, the silane containing MIP shows a very porous structure whereas EGDMA containing MIP layer failed to show any porosity. As shown in Fig. 3, in polymer adduct having template inside the matrix smooth surface is visible, due to absence of any cavity in the polymer film. Whereas, template extraction leads to more porous surface due to removal of template from polymer matrix resulting in the creation of cavities in the polymer.

3.4. Role of TEOS as cross-linker

To explore the role of silane-cross-linked polymer in template extraction DPV analysis was performed. Fig. 4 shows DPV runs of metformin (1.0 ng mL^{-1}), at silane-cross-linked polymer, EGDMA-cross-linked polymer and NIP-modified electrodes. As depicted in Fig. 4, runs 1–3, highest current response was found with the silane-cross-linked polymer modified electrode, whereas negligible current was found on NIP-modified electrode. After immersing these electrodes in extraction solvent (0.1 M NaOH, 0.5 mL for 20 min), complete template removal was observed from silane-cross-linked polymer (run 4), whereas, EGDMA-cross-linked polymer, still retain some template molecules in the polymer matrix (run 5). From this observation, it can be easily concluded that the problem of difficult template washing from the compact imprinted polymer matrix can be easily tackled using silane compounds as cross-linker in the place of the other popular cross-linkers like EGDMA.

3.5. Electrochemical behavior of metformin

Preliminary cyclic voltammetric experiments were carried out to study the metformin voltammetric behavior at the bare and MIP-modified electrodes. The oxidation system is characterized by an anodic peak at the positive-moving step and by the absence of any cathodic peak on the reverse scan, indicating that the oxidation is irreversible (Fig. 5A). In brief, the electrochemical oxidation of an imino-group in guanidino-compounds i.e. metformin to an N-hydroxyimino-group produced the oxidation peak. Then most of the N-hydroxyimino-group fast hydrolyzed to a carbonyl imino-group, a stable compound giving an irreversible oxidation of metformin [29].

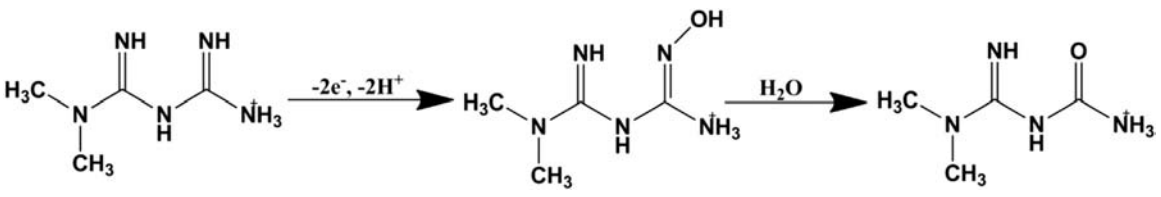

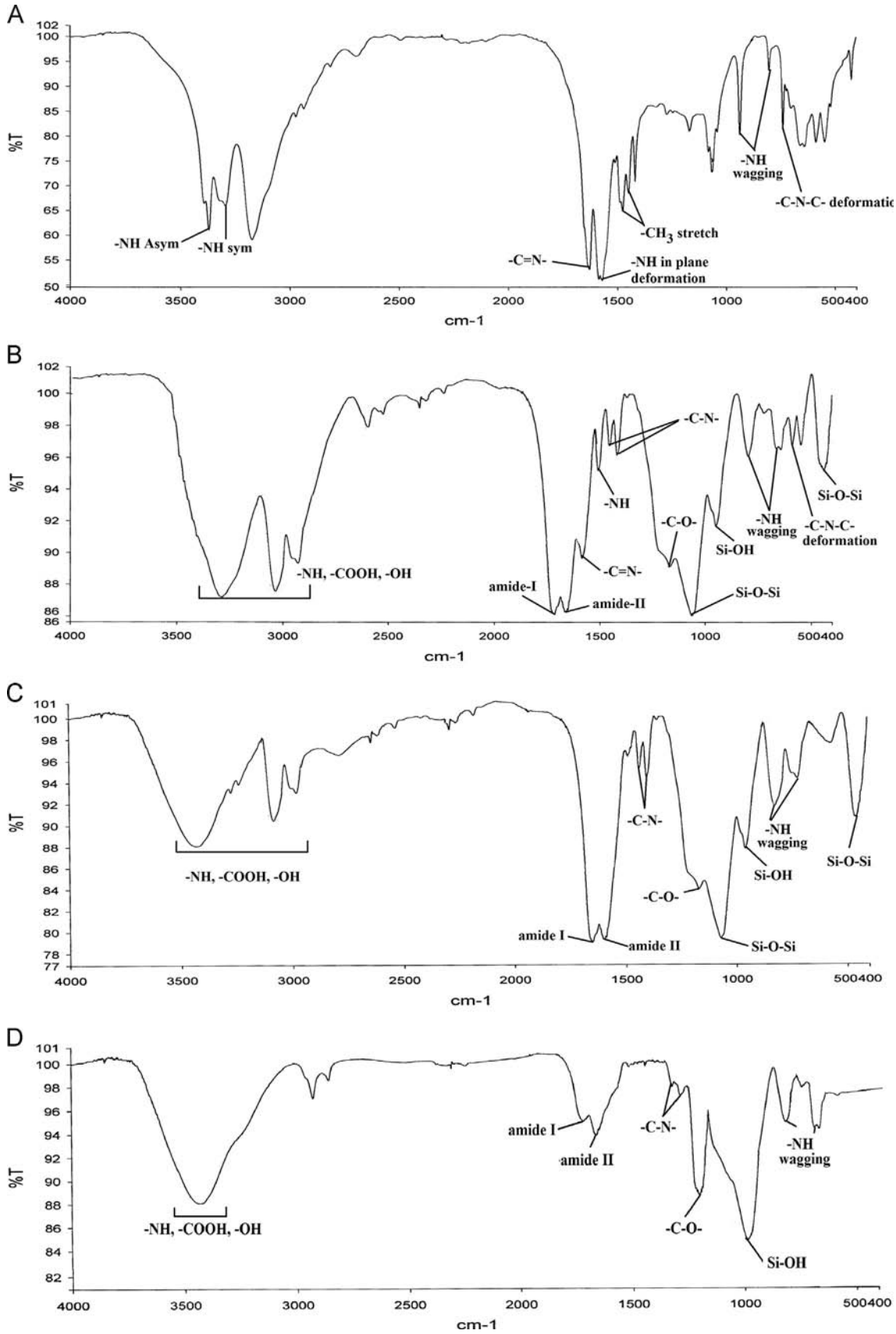

Fig. 2. IR spectra of template (curve A), adduct with AuNPs (curve B), MIP (curve C) and MIP without AuNPs (curve D).

CV runs of metformin (1.0 ng ml^{-1}) have been taken at various scan rates (0.02–0.10 V s^{-1}) with accumulation potential −0.4 V and accumulation time 250 s at pH 7.5 (optimization of analytical parameters are discussed in SI-Section 1.3), as shown in Fig. 5A. This suggest an ir-reversible oxidation of electro-active metformin. CV runs bear linear relationships between peak current (I_p) and

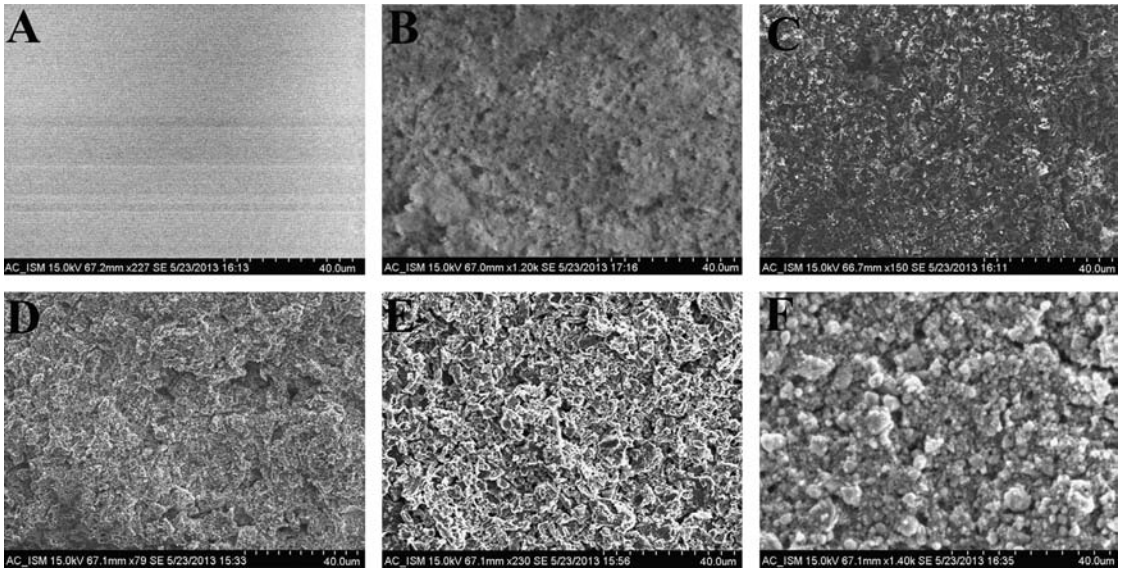

Fig. 3. SEM images for bare (A) and polymer modified Pt electrode surfaces using different conditions, (B) adduct in the presence of EGDMA, (C) adduct in the presence of sol–gel with AuNPs, (D) adduct in the presence of sol–gel without AuNPs, (E) MIP in the presence of EGDMA and (F) MIP in the presence of sol–gel with AuNPs.

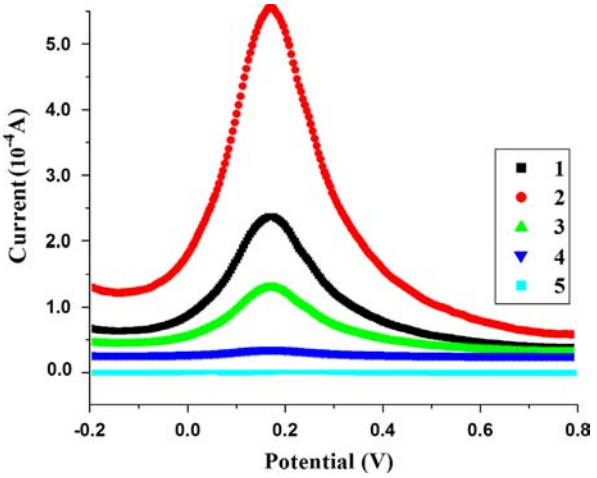

Fig. 4. DPV current response for metformin on EGDMA-cross-linked polymer (1 and 3), silane-cross-linked polymer (2 and 5) and NIP (4) modified Pt electrodes before and after treatement with extraction solvent (0.1 M NaOH).

scan rate (υ) which confirms an adsorption controlled mechanism (Fig. 5A, inset).

$$I_p = (5.51 \times 10^{-4} \pm 1.68 \times 10^{-5})v + (7.83 \times 10^{-6} \pm 1.09 \times 10^{-6}),$$

$$n = 9,\ R^2 = 0.998$$

whereas the peak current does not show such linear relationship with square root of scan rate:

$$I_p = (2.53 \times 10^{-4} \pm 1.67 \times 10^{-5})v^{1/2} + (1.9 \times 10^{-5} \pm 4.08 \times 10^{-6}),$$

$$n = 9,\ R^2 = 0.986$$

This linear relationship indicates that diffusion mechanisms are also involved in the electrochemical reaction and the major process for analyte transport to the electrode surface is both adsorption as well as diffusion-controlled. In the present study the effect of scan rate on the cathodic peak potential was also investigated. The peak potential shifts to more negative values with increasing scan rate (Fig. 5A, inset). The relationship between the peak potential and the logarithm of the scan rate was

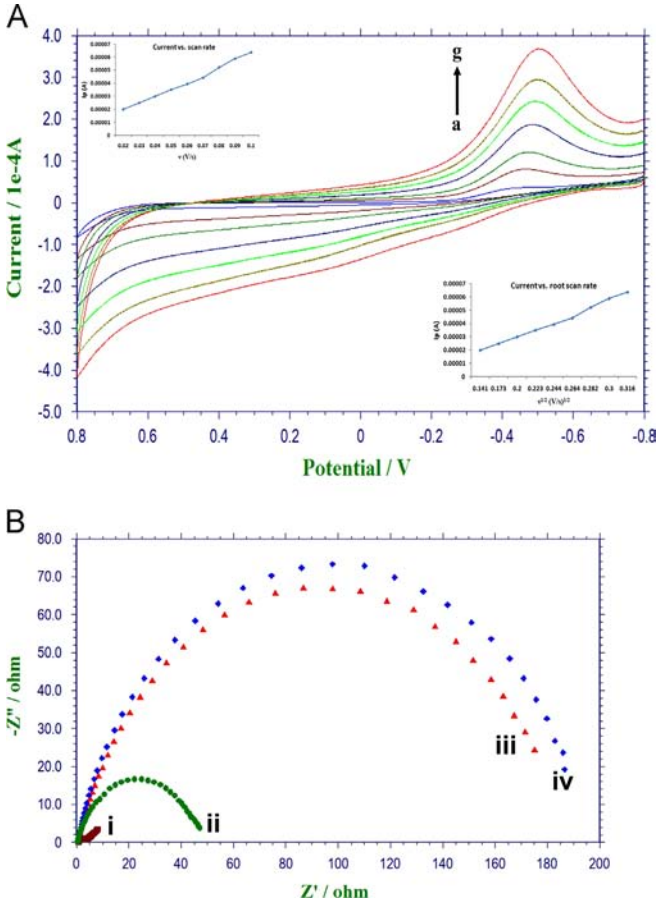

Fig. 5. (A) Cyclic voltammogram of metformin (1.0 ng ml^{-1}) at various scan rates (0.02–0.09 V s^{-1}) with linear equation graph between current vs. scan rate and current vs. square root of scan rate (inset); (B) EIS spectra for bare (i), MIP (ii), adduct with 85 ng ml^{-1} template and NIP (iv) modified Pt electrodes.

expressed by the following equation:

$$E_p(V) = (-0.106 \pm 0.001)\log\ v + (-0.621 \pm 0.001),$$
$$n = 9,\ R^2 = 0.999$$

Potential shifting with scan rate supports the irreversibility of the electrochemical reaction under investigation. Peak potential of an ir-reversible process obeys the following equations [30]:

$$\alpha n = \frac{1.857RT}{F(E_p - E_{p/2})} \quad (2)$$

$$E_p = E_{p/2} - b[0.52 - 0.5\log\frac{b}{d} - \log k_s + 0.5 \log v] \quad (3)$$

$$b = \frac{2.303RT}{\alpha nf} \quad (4)$$

where α=electron transfer co-efficient, n=no. of electron, E_p=peak potential, D=diffusion co-efficient, and υ=scan rate. In order to determine the rate constant i.e. k_s of the process, it is necessary to find out α, n and D values.

Chronocolumetry technique is applied to calculate the surface coverage (Γ^0) and diffusion coefficient (D) of the analyte. According to the integrated Cottrell equation, the relation between charges (Q) vs. square root of time ($t^{1/2}$) can be described as follows [31]:

$$Q = 2nFAC(Dt)^{1/2}\pi^{-1/2} + Q_{ads} + Q_{dl} \quad (5)$$

$$Q_{ads} = nFAT^0 \quad (6)$$

$$I_p = \frac{n^2F^2\Gamma^0A\vartheta}{4RT} \quad (7)$$

where A is the geometrical area of electrode that is (3.14×10^{-2} cm^2), C is the concentration (1.0 ng ml^{-1}) of metformin, Q_{dl} is the double layer charge, Q_{ads} is the Faradaic oxidative charge and other symbols have their usual meanings. For metformin–MIP, Q_{dl} and total charge ($Q_{dl}+Q_{ads}$) is evaluated from the respective intercepts of the Anson plots (Q vs. $t^{1/2}$) in the absence and presence of metformin. The values of n and Γ^0 can be obtained as 2.0 and 8.85×10^{-10} mol cm^{-2}, respectively using Eqs. (5–7). In the present instance, Γ^0 reflects the total surface coverage of metformin analyte (2.778×10^{-11} mol or 1.673×10^{13} molecules) specifically bound to MIP cavities (each molecule per cavity). From the slope of the Anson plot, diffusion coefficient can be calculated for metformin and is found to be 3.941 cm^2 s^{-1}. The estimated values of α and k_s for the oxidation of metformin at MIP-modified Pt electrode were found to be 0.1986 and 0.232 cm s^{-1}, respectively using Eqs. (2–4). The lower value of α (<0.5) suggests the ir-reversibility of the process, whereas the higher value of k_s indicates a fast kinetics due to the role of MIP-cavities present at the electrode surface.

Fig. 5B illustrates the typical results of electrochemical impedance spectra (presented in the form of the Nyquist plot) of the bare (curve i), MIP- (curve ii), MIP-after rebinding with template (curve iii) and NIP- (curve iv) modified Pt electrodes, respectively. It is obvious that the bare electrode exhibits a straight line, which reveals that there is almost no heterogeneous charge-transfer resistance on the bare surface, while the R_{ct} of the NIP-layer is much larger, indicating that the compact film of low conductivity acts as a definite kinetic barrier for the charge transfer [32]. Similar to the NIP-, the R_{ct} of the MIP-after rebinding with metformin (in their saturated stage) also higher because metformin molecules occupy imprinted molecular cavities, which make them a highly compact structure. Therefore, cavities are unavailable for the template molecule to diffuse through. A significant decrease in R_{ct} can be observed on the MIP-layer because the cavities in the film are not occupied by the template and are, therefore, available for the charge transfer.

3.6. Computational study of redox mechanism

Theoretical and experimental studies have shown the importance of quantum-chemical process in understanding the electrochemical mechanistic aspects of numerous organic compounds. The frontier orbitals are of extreme importance for the evaluation of molecular reactivity. Initially, calculation of frontier molecular orbital HOMO (highest occupied molecular orbital) and LUMO (lowest unoccupied molecular orbital) of the metformin was performed. More negative the energy of the HOMO, more susceptible is

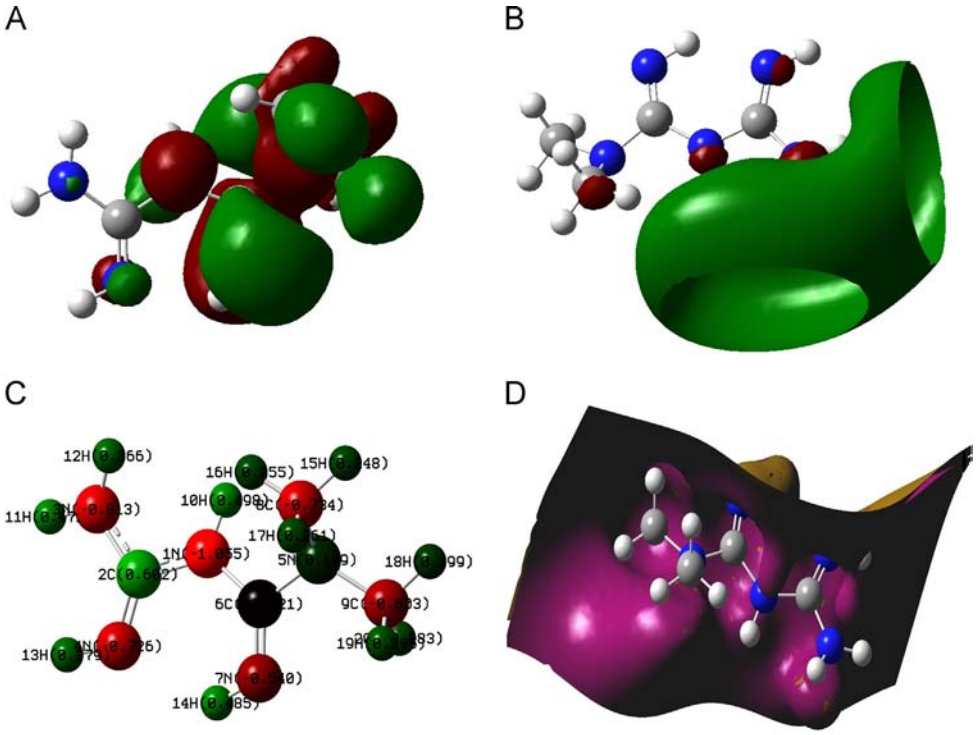

Fig. 6. Images of (A) HOMO, (B) LUMO, (C) Mulliken charge distribution and (D) electrostatic potential surface of metformin molecule.

the molecule to donate electrons and, consequently, higher is the tendency to suffer oxidation [33]. As depicted in Fig. 6 A and B, metformin possesses a lower HOMO (−0.344 Hartree or −903.1718 kJ mol^{-1}) and higher LUMO (0.026 Hartree or 68.2629 kJ mol^{-1}) energy i.e. molecule is prone to oxidation. Similarly, the calculations of the Mulliken charge are widely used to identify the set of atoms that has a greater tendency to undergo oxidation, based on the distribution of the orbitals HOMO on the molecule (Fig. 6, C and D) [33]. According to the theoretical model, more negative the value obtained, greater the tendency to donate electrons and hence greater the possibility of the occurrence of the oxidation reaction. Our result shows that the nitrogen atom close to the primary amine has more negative charge, indicating that the oxidation would occur most probably to/with this atom. The computational data shows a good agreement with the results obtained by electrochemical analysis.

3.7. Estimation of metformin

Herein, DPV was employed for the quantitative determination of metformin, on MIP-modified-Pt electrode, which is relatively sensitive compared to the conventional CV method. As shown in Fig. 7, the DPV peak current increases with the increase in concentration of metformin, which suggests that more and more binding sites in the film are occupied by metformin molecules. The relative current change tended to be constant till the concentration of metformin was 85.0 ng mL^{-1}, which indicates that metformin molecules gradually occupy the imprinting sites and approached the point of 'saturation'. The calibration curve for the DPV peak current observed for metformin oxidation versus metformin concentration at MIP electrode shows linearity over a concentration range of 0.020–80.0 ng mL^{-1}. The calibration linear equation of current vs. concentration of metformin i.e. I_p ($10^{-4}A$) $=(2.8421\times10^{-4}\pm1.3369\times10^{-4})+(6.2346\times10^{-6}\pm4.3438\times10^{-6})C$, $n=9$, ($R^2=1.0$) was obtained in the optimal conditions (Fig. 7B, inset). The experimental detection limit was obtained to be 0.005 ng mL^{-1}.

The result obtained by the proposed method was compared with an earlier reported method (copper-loaded activated charcoal modified electrode for metformin detection, LOD=9.0 nM) [29]. To validate the proposed method, *F*-test and *t*-test were conducted and the calculated values were 4.12 and 0.98, which were less than the theoretical ones (obtained at 95% confidence limit, $n_1=5$, $n_2=5$) of 5.05 and 2.07, respectively. These indicated that there were no significant difference between the proposed and earlier reported method [29] but our sensor is approximately 230 times more sensitive than previous one.

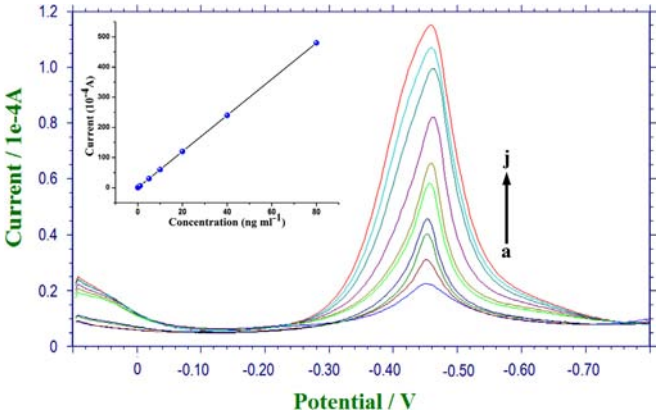

Fig. 7. Differential pulse voltammograms obtained during successive increments of metformin (a–j) with inset showing the corresponding calibration curve.

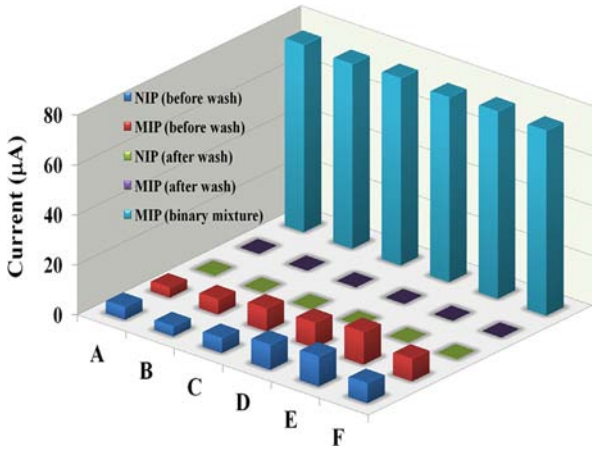

Fig. 8. DPV response for interferents, when studied individually (each 5.0 ng mL^{-1}): (A) urea, (B) ascorbic acid, (C) glucose, (D) uric acid, (E) biguanidine and (F) some ions (K^+, Na^+, Ca^{+2} and Cl^-) on MIP and NIP-modified electrodes before and after water washing and in binary mixture of metformin (1.0 ng mL^{-1}) and interferents (1000 ng mL^{-1}).

3.8. Cross-reactivity study

The selectivity of the MIP electrode in this work was evaluated in the presence of different interfering molecules commonly present in human blood (Fig. 8). Voltammetric response of metformin imprinted polymer and NIP-modified electrodes were examined in the presence of these interfering substances like urea (A), ascorbic acid (B), glucose (C), uric acid (D), biguanide (E, structural analog of metformin) and some ions (F; K^+, Na^+, Ca^{+2} and Cl^-). Both MIP and NIP (before washing)-modified electrodes were exhibit small current for some of the interferents, when studied individually (Fig. 8). However, such contributions on MIP- and NIP-based sensor must be due to non-specific interaction, which could easily be curtailed simply by water-washings ($n=3$, 0.5 mL) (Fig. 8). A parallel cross-reactivity of binary mixtures of interferents (taken in the 1:1000 concentration ratio with metformin) was also studied on MIP-modified electrode (Fig. 8). As depicted in the figure, the sensor shows 100% current response for template molecule even in the presence of very high concentration of interferents. Based on the above observations, we can conclude that the recognition sites formed in the polymerized film have the capability to distinguish target molecules through their size, shape and functional group distribution.

3.9. Reproducibility, repeatability, ruggedness and storage stability of the imprinted sensor

To investigate the reproducibility of the proposed sensor during fabrication, three sensors were fabricated independently under the same conditions and examined in the presence of metformin (1.0 ng ml^{-1}). The response shows a relative standard deviation (RSD) of 1.8%, indicating an excellent reproducibility during electrode fabrication. To explore the repeatability of the proposed sensor six consecutive runs were taken for same concentration of metformin (1.0 ng ml^{-1}) and the calculated RSD was found to be about 0.9%. It was observed that the current as well as potential of the peak related to the metformin electro-oxidation does not change significantly. This indicates that the proposed sensor could be regenerated and used repeatedly. After the electrode was stored for 45 days, it retains 94.6% of its original response, suggesting acceptable storage stability of the sensor.

Table 3
Real world applicability of the proposed sensor.

S.N.	Sample	Added ($ng\ ml^{-1}$)	Found ($ng\ ml^{-1}$)	Recovery (%)	RSD (%) ($n=3$)
1.	Unknown	–	0.5620	–	–
2.	Spike 1	2.0	2.6000	101.4	1.8
3.	Spike 2	4.0	6.6220	100.9	2.1
4.	Spike 3	8.0	14.5412	99.9	1.1

3.10. Determination of metformin in pharmaceutical sample

To investigate the real world application of the MIP sensor, it was applied to determine metformin in a pharmaceutical drug, very commonly used for diabetic patient (Table 3). Before adding a standard solution of metformin, the voltammetric base line of the pharmaceutical medium was measured and a DPV signal was found in the studied potential window at the same potential as reported for metformin peak, indicating that there are no significant interferences from inorganic cations, anions and some organic substances found in pharmaceutical preparations (tablets). To assess the suitability of the method recovery experiments were also performed, by use of standard additions. Recoveries ranged from 98.8 to 100.2%, indicates the accuracy and repeatability of the proposed method in real sample.

4. Conclusions

In this work, we have successfully synthesized the MIP for metformin using acrylamide and acrylic acid as monomer and TEOS as cross-linker. Herein, dual action of AuNPs: (1) as oxygen donor for hydrolysis and condensation of silane and (2) as enhancer for electro-conductivity were effectively explored. To optimize the property of imprinted polymer various concentration of AuNPs, monomers and cross-linker were used. The kinetic parameters involved in the electro-oxidation process (such as the transfer coefficient, rate constant and the diffusion coefficient) were also evaluated. The very low LOD value and high levels of repeatability and reproducibility obtained in proposed sensor allowed the direct application of this methodology in the electro-analysis of metformin in trace concentrations, without any clean-up step.

Acknowledgment

Authors are thankful to the Department of Science and Technology, Government of India for sanction of Fast Track Research Project for Young Scientists to Dr. Rashmi Madhuri (Ref. no.: CS-381/2012) and Dr. Prashant K. Sharma (Ref. no.: SR/FTP/PS-157/2011). Dr. Prashant K. Sharma is also thankful to Indian School of Mines, Dhanbad for Grant of Major Research Project under Faculty Research Scheme. E.R. and S.P. is also thankful to Indian School of Mines, Dhanbad for Junior Research Fellowship.

Appendix. Supplementary material

Supplementary data associated with this article can be found in the online version at http://dx.doi.org/10.1016/j.talanta.2013.11.074.

References

[1] C.R. Thomas, S.L. Turner, W.H. Jefferson, C.J. Bailey, Biochem. Pharmacol. 56 (1998) 1145–1150.
[2] J.A. Johnson, S.R. Majumdr, S.H. Simpson, E.L. Toth, Diabetes Care 25 (2002) 2244–2248.
[3] L. Zhang, Y. Tian, Z. Zhang, Y. Chen, J. Chromatogr. B 854 (2007) 91–98.
[4] R.Q. Gabr, R.S. Padwal, D.R. Brocks, J. Pharm. Sci. 13 (2010) 486–494.
[5] P. Umapathi, J. Ayyappan, S.D. Quine, Trop. J. Pharm. Res. 11 (2012) 107–116.
[6] M.S. Lennard, C. Casey, G.T. Tucker, H.F. Woods, Br. J. Clin. Pharmacol. 6 (1978) 183–185.
[7] S.Y. Feng, E.P.C. Lai, E.D. Zlotorzynska, S. Sadeghi, J. Chromatogr. A 1027 (2004) 155–160.
[8] M.R. Ganjali, P. Norouzi, M. Zare, Russ. J. Electrochem. 44 (2008) 1135–1143.
[9] X.-J. Tian, J.-F. Song, X.-J. Luan, Y.-Y. Wang, Q.-Z. Shi, Anal. Bioanal. Chem. 386 (2006) 2081–2086.
[10] S. Skrzypek, V. Mirceski, W. Ciesielski, A. Sokołowski, R. Zakrzewski, J. Pharm. Biomed. 45 (2007) 275–281.
[11] X.-J. Tian, J.-F. Song, J. Pharm. Biomed. Anal. 44 (2007) 1192–1196.
[12] N. Sattarahmady, H. Heli, F. Faramarzi, Talanta 82 (2010) 1126–1135.
[13] J.Z. Song, H.F. Chen, S.J. Tian, Z.P. Sun, J. Chromatogr. B 708 (1998) 277–283.
[14] J.M. Calatayud, P.C. Falco, M.C.P. Marti, Anal. Lett. 18 (1985) 1381–1390.
[15] F. Tache, V. David, A. Farca, A. Medvedovici, Microchem. J. 68 (2001) 13–19.
[16] J. Keal, A. Somogyi, J. Chromatogr. B 378 (1986) 503–508.
[17] S. AbuRuz, J. Millership, J. MaElnay, J. Chromatogr. B 798 (2003) 203–2009.
[18] B.L. Kolte, B.B. Raut, A.A. Deo, M.A. Bagool, D.B. Shinde, J. Chromatogr. B 788 (2003) 37–44.
[19] S. AbuRuz, J. Millership, J. MaElnay, J. Chromatogr. B 817 (2005) 277–286.
[20] O. Vesterqvist, F. Nabbie, B. Swanson, J. Chromatogr. B 716 (1998) 299–304.
[21] S. Majdi, A. Jabbari, H. Heli, H. Yadegari, A.A. Moosavi-Movahedi, S. Haghgoo, J. Solid State Electrochem. 13 (2009) 407–416.
[22] G. Vasapollo, R.D. Sole, L. Mergola, M.R. Lazzoi, A. Scardino, S. Scorrano, G. Mele, Int. J. Mol. Sci. 12 (2011) 5908–5945.
[23] L. Chen, S. Xuab, J. Li, Chem. Soc. Rev. 4 (2011) 2922–2942.
[24] A. Simón de Dios, M.E. Díaz-García, Anal. Chim. Acta 666 (2010) 1–22.
[25] J.N. Hay, H.M. Raval, Chem. Mater. 13 (2001) 3396–3403.
[26] S. Miertus, E. Scrocco, J. Tomasi, Chem. Phys. 55 (1981) 117–129.
[27] S. Rho, S.J. Kim, S.C. Lee, J.H. Chang, H.-G. Kang, J. Choi, Curr. Appl. Phys. 9 (2008) 534–537.
[28] D.A. Skoog, F.T. Holler, T.A. Neiman, Principles of Instrumental Analysis, fifth ed., Harcourt Brace College Publishers, Orlando, 1998.
[29] M.B. Gholivand, L. Mohammadi-Behzad, Anal. Biochem. 438 (2013) 53–60.
[30] E. Laviron, J. Electroanal. Chem. 10 (1979) 19–28.
[31] A.J. Bard, L.R. Faulker, Electrochemical Methods, second ed., Wiley, NewYork, 2001.
[32] J. Li, J. Zhao, X. Wei, Sens. Actuators B 140 (2009) 663–669.
[33] T.M.B.F. Oliveira, F.W.P. Ribeiro, J.M. de Nascimento, J.E.S. Soares, V.N. Freire, H. Becker, P. de Lima-Neto, A.N. Correia, J. Braz. Chem. Soc. 23 (2012) 110–119.